JOURNAL OF MATERIALS SCIENCE **36** (2001) 3699–3705

Sputter-deposited Ti oxide films used for photoelectrocatalytic degradation of 4-chlorophenol

J. RODRÍGUEZ*, M. GÓMEZ*, G. A. NIKLASSON
Department of Materials Science, The Ångström Laboratory, Uppsala University, P.O. Box 534, SE-751 21 Uppsala, Sweden

S.-E. LINDQUIST
Department of Physical Chemistry, Uppsala University, P.O. Box 532, SE-751 21 Uppsala, Sweden

C. G. GRANQVIST
Department of Materials Science, The Ångström Laboratory, Uppsala University, P.O. Box 534, SE-751 21 Uppsala, Sweden
E-mail: claes-goran.granqvist@angstrom.uu.se

Ti oxide films were made by reactive magnetron sputtering under conditions yielding "penniform" structures with large porosity. X-ray diffractometry showed that rutile-like and anatase-like films were produced depending on the oxygen content in the sputter plasma. Rutherford backscattering spectrometry documented some oxygen overstoichiometry. Spectral optical measurements were used to analyze the absorption around the fundamental band gap and to give evidence of some hydration and hydroxylation in the films. The various Ti oxide films were brought in contact with 4-chlorophenol (4-CP), whose photo-electrocatalytically induced degradation under ultraviolet irradiation was investigated in a reactor allowing optical probing of 4-CP as well as of intermediate reaction products such as benzoquinone. A rutile-like structure was conducive to the degradation of 4-CP, which can be reconciled with the band gap being suitable for producing photoinduced holes capable to effecting oxidation of the pollutant.

1. Introduction

Heterogeneous photocatalysis is a subject of large and increasing importance [1–5]. It can be used for the decomposition of hazardous wastes as well as for antibacterial surface treatment [6, 7], self cleaning [8, 9], antifogging [10], etc. Titanium dioxide stands out as the primary material for these applications. The great majority of the work thus far has been devoted to surfaces made by colloidal techniques, but recent work [11–14] has demonstrated that reactive magnetron sputtering is a viable and versatile technique. The present work expands our earlier endeavors related to sputtered Ti oxide for the photodegradation of an organic pollutant [14], as well as for solar cell applications [15], and is devoted to the influence of the sputtering conditions, and hence the composition and structure, of Ti oxide surfaces.

The Ti oxide films of present interest are characterized by their energy bands being appropriate for water purification [3] as well as by their great porosity which renders them capable of having a very large interface to a fluid. The photocatalysis involves excitation of an electron from the valence band to the conduction band; the remaining hole migrates under the influence of the electric field towards the surface of the semiconductor and reaches a site where it can oxidize an electron donor associated with the pollutant. With the object of understanding the factors contributing to the photocatalytic activity associated with Ti oxide, several groups have carried out photocatalytic mineralization studies using the two common crystal phases of Ti oxide, i.e., anatase and rutile [16, 18]. In the photomineralization of phenol sensitized by anatase and rutile Ti oxide, it has been reported [16, 17] that rutile is inactive as a photocatalyst. However Sclafani *et al*. [18], in studies of the same photosystem, showed that rutile is active or inactive depending on the initial conditions used to chemically prepare the Ti oxide.

The positions of the energy bands are important for the photocatalysis; they can be changed with respect to an electrolyte by altering its pH. The Fermi level of the Ti oxide can be modified by doping with transition metal ions [19] and—most importantly for the present study—by achieving non-stoichiometry through a variation of the density of oxygen vacancies [20], thereby creating a band of electron states between

* Present and permanent address: Universidad Nacional de Ingenieria, Facultad de Ciencias, Av. Tupac Amaru S/N, Casilla Postal 31-139, Lima, Peru.

the conduction band and the Fermi level. These states have a dramatic influence on the electrical properties.

This paper is organized so that Section 2 below discusses thin film fabrication. Section 3 then covers film characterization with respect to composition and structure, and Section 4 treats film characterization by optical measurements. Section 5 is devoted to measurements of the photocatalytic effect of substoichiometric Ti oxide films in contact with a solution containing 4-chlorophenol [4-CP]. Specifically we study *in situ* absorbance spectra taken at different degradation times and find enhanced degradation rates of 4-CP in films with low oxygen content. These results are correlated with a shift of the fundamental absorption band to larger wavelengths. The main results are summarized in Section 6.

2. Film preparation

Ti oxide films were deposited using reactive DC magnetron sputtering in a system based on a Balzers UTT 400 vacuum chamber [21]. The targets were 5-cm-diameter metallic plates of Ti (99.9%). The chamber was evacuated to $\sim 1.3 \times 10^{-5}$ Pa by turbo molecular pumping. Prior to sputter deposition, Ar (99.998%) and O_2 (99.998%) gas were mixed and introduced via separate mass-flow-controlled inlets. The O_2/Ar gas flow ratio was kept constant at a value Γ lying between 0.069 to 0.078 in order to achieve different compositions and structures. The pressure in the sputter plasma was $\sim$1.6 Pa.

The films were deposited onto carbon, glass substrates, as well as glass precoated with a layer of transparent and conducting ITO (i.e., In_2O_3:Sn) having a resistance/square of 20 Ω. The substrates were kept at 250°C during deposition. Film uniformity was assured by rotating the substrate during the deposition, and this rotation also led to a suitable "penniform" microstructure, as discussed in some detail elsewhere [22]. The film thickness d was determined by surface profilometry using a Tencor Alpha-Step 200 instrument; values are shown in Table I. Deposition rate was obtained by dividing d by sputtering time. Typically, the rate was 0.5 nm/s, with the exception of samples deposited at the highest oxygen admixtures for which the deposition rate was approximately 0.4 nm/s.

3. Film characterization: Composition and structure

The composition of the Ti oxide films is expected to be of critical importance for their photo-electrochemical properties, including their photocatalytic ability, and in earlier work we showed that the photoelectrical effect was influenced by having different magnitudes of Γ during the thin film deposition [15, 23]. For the present films, we used Rutherford Backscattering Spectrometry (RBS) to determine the elemental composition of films deposited onto carbon. We used the facilities of the Tandem Laboratory of Uppsala University.

TABLE I Data for the Ti oxide films, showing O_2/Ar gas flow ratio during sputtering Γ and film thickness d. Also given are the fundamental band gap E_g and the paramenters Σ, a_o, E_o and ΔE used to fit our optical data to Eqs. (2) and (3)

Γ	d (nm)	E_g (eV)	Σ (eV)	a_o (cm^{-1})	E_o (eV)	ΔE (eV)
0.069	624	3.24	0.08	4209	2.99	0.58
0.071	620	3.24	0.08	3815	2.99	0.59
0.073	618	3.25	0.08	3179	2.99	0.58
0.075	579	3.26	0.08	3361	2.99	0.57
0.078	427	3.36	0.07	1150	2.99	0.66

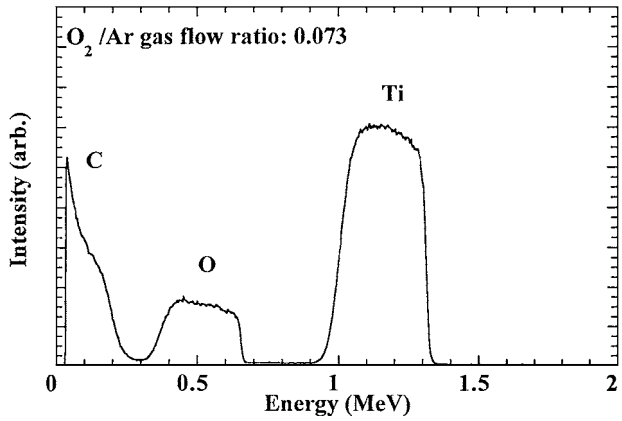

Figure 1 Rutherford backscattering spectroscopy data for a 618-nm-thick Ti oxide film made by sputtering at the shown O_2/Ar gas flow ratio. The broad peaks stem from the shown atomic species in the film, and the low-energy feature originates from the carbon substrate.

Fig. 1 illustrates a typical RBS spectrum. It shows well defined and characteristic features corresponding to the carbon substrate as well as to oxygen and titanium in the films. The RBS data were consistent with a composition TiO_{2+z} with $z \approx 0.1$ for all films. The small overstoichiometry, i.e., the fact that z is positive, is likely to be caused by strongly bound water molecules or hydroxyl groups. A similar excess of oxygen is commonly observed in sputter deposited porous films [24–26].

The crystalline structure of the Ti oxide films was studied by X-ray diffraction (XRD) using a Siemens D5000 diffractometer with Cu anode and grazing incidence unit. Data from TiO_2 standards [27] were used to identify the diffraction peaks. Fig. 2 shows grazing incidence X-ray diffractograms for Ti oxide films sputter deposited at different values of Γ onto glass substrates.

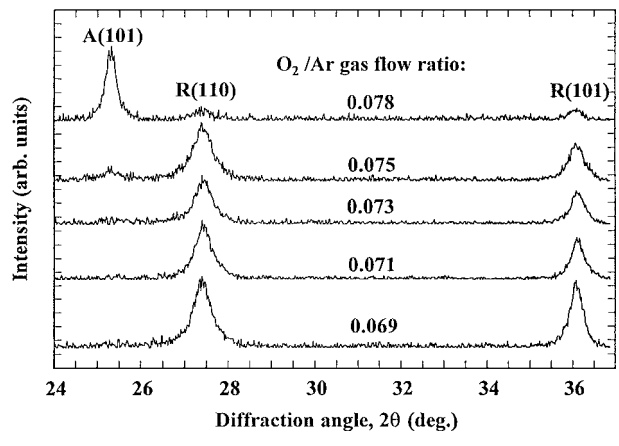

Figure 2 X-ray diffractograms for Ti oxide films made by sputtering at the shown O_2/Ar gas flow ratios. The peaks originate from the stated reflections in the anatase (A) and rutile (R) structures.

For $\Gamma = 0.069$, the diffractograms display two prominent peaks due to the rutile (110) and (101) reflections, apparent at diffraction angles 2θ being 27.4° and 36.1°, respectively. No evidence of the anatase phase was observed. For increasing Γ, the intensity of the rutile features decreased and an anatase (101) peak appeared at $2\theta = 25.3°$. Clearly a large amount of oxygen in the sputter plasma promotes the formation of the anatase structure.

The mean grain size D for the films was estimated from the XRD data by applying Scherrer's formula, i.e.,

$$D = \frac{K\lambda_x}{\beta \cos\theta}, \tag{1}$$

where K is a dimensionless constant, λ_x is the X-ray wavelength, and β is the full width at half maximum of the diffraction peak. Applying this formula to the rutile (101) peak for films deposited at $\Gamma = 0.069$, the grain size was found to be ~25 nm, and for films deposited at $\Gamma = 0.078$ the grain size was ~32 nm as derived from the anatase peak.

An influence of the gaseous ambience on the preferred crystalline growth has been reported before, and it is believed that there is a tradeoff between the ion/atom impact angle to the substrate, which leads to a preferential growth of crystalline planes capable of facile ion channeling [28, 29], and thermodynamic parameters such as surface free energy [30]. Our films displayed a preferred crystalline growth with the (110) and (101) rutile planes parallel to the surface in the case of low oxygen pressures; these are planes characterized by low surface free energy [30]. At higher oxygen pressures, the intensity of the (110) and (101) rutile peaks decrease, which agrees with reported data [30], and a peak associated to the anatase is observed. The anatase structure has a lower density than the rutile structure, and it is expected that the former of these is produced at high gas pressures.

4. Film characterization: Optical properties

Total reflectance R and transmittance T of the Ti oxide films deposited on glass were recorded in the $300 < \lambda < 2500$ nm wavelength range with a Perkin-Elmer Lambda 9 double beam spectrophotometer equipped with an integrating sphere. The measurements of R and T of films deposited onto glass were performed at near normal incidence (8°) and at normal incidence, respectively. The reflectance measurements used a $BaSO_4$ plate as reference.

Optical constants were calculated by using a combination of direct inversion of Fresnel's equations for a thin film on a substrate (RT method [31]) and the Forouhi Bloomer (FB) technique [32]. The latter approach uses a simple parametrization for the extinction coefficient k and obtains the refractive index n via Kramers-Kronig analysis. Details of the calculation method can be found elsewhere [32, 33]. The solid curves in Fig. 3 shows experimental R and T for a typical 618-nm-thick Ti oxide film deposited at $\Gamma = 0.073$. The transmittance and reflectance of the bare substrate

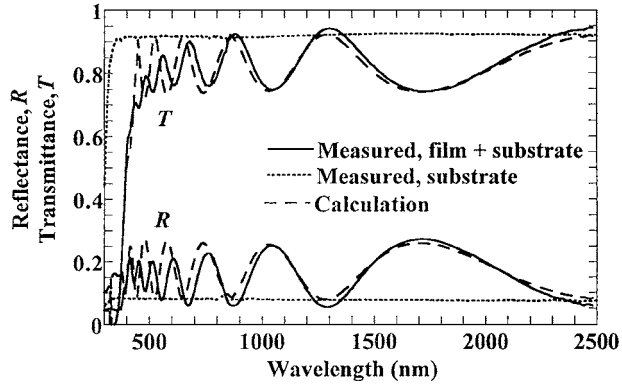

Figure 3 Spectral reflectance and transmittance as measured and calculated for a sputter deposited Ti oxide film on a glass substrate and for the bare substrate. Data are given also from a calculation using evaluated optical constants.

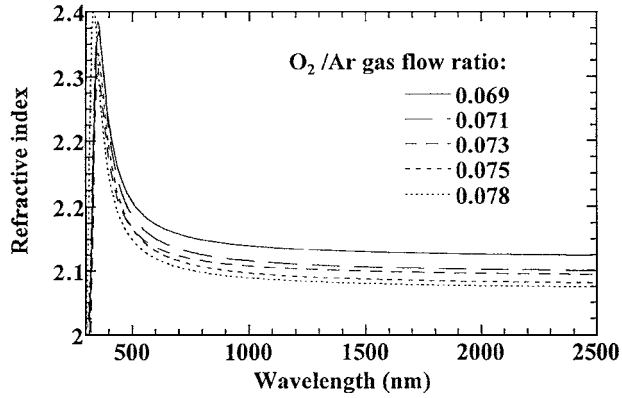

Figure 4 Spectral refractive index for Ti oxide films made by sputtering at the shown O_2/Ar gas flow ratios.

are shown as dotted curves. Our data indicate a peculiar characteristic attributed to inhomogeneities in the film, namely that T and R of the film/substrate configuration are higher than the transmittance and lower than the reflectance of the bare substrate in the region of transmittance maxima and reflectance minima, respectively. For $\lambda < 700$ nm, the interference fringes become less pronounced due to the onset of absorption. Calculated data, shown as dashed curves in Fig. 3, were obtained by using the evaluated n and k; these results, which agree well with the measurements, serve as an internal check on the evaluation of the optical constants.

Values of n and k for films made at different magnitudes of Γ are given in Figs. 4 and 5, respectively. Fig. 4 shows that the refractive index is ~2.1 at $\lambda = 2500$ nm for the rutile type film obtained at $\Gamma = 0.069$, and that n decreases markedly when the oxygen admixture was increased. In the case of k for $300 < \lambda < 450$ nm, Fig. 5 shows that the peak is shifted towards shorter wavelengths for enhanced Γ. This observation is consistent with the promotion of the anatase structure, which is known [3] to have a fundamental band gap that is larger than for rutile. It is also observed that k is large at short wavelengths. We note that recent studies have shown that the influence of the oxygen partial pressure on the structure and optical properties of Ti oxide films are in agreement with our results [34, 35]. On the other hand Mikula *et al.* [13] gave evidence for a decrease of the

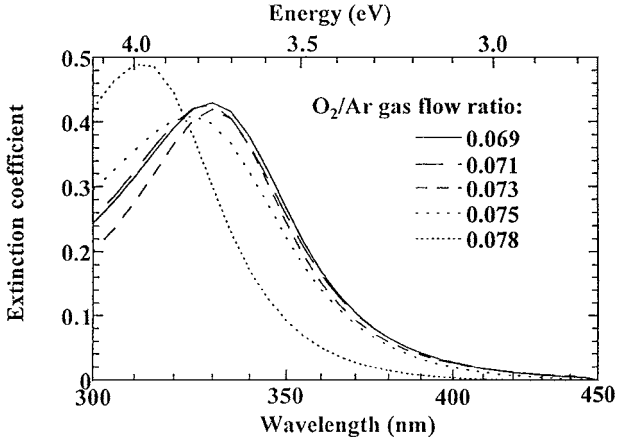

Figure 5 Spectral extinction coefficient for Ti oxide films made by sputtering at the shown O_2/Ar gas flow ratios.

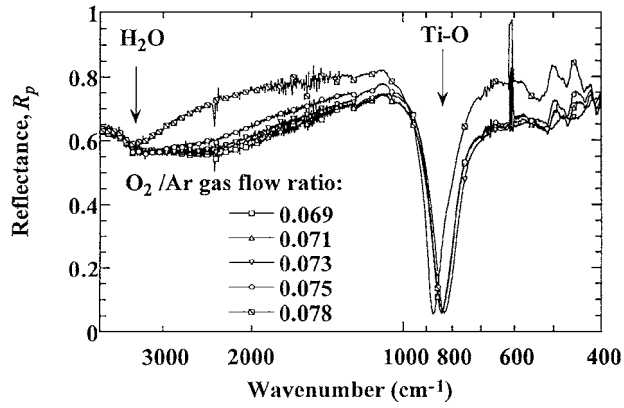

Figure 6 Spectral reflectance of p-polarized light at 60° incidence angle for Ti oxide films made by sputtering at the shown O_2/Ar gas flow ratios. Arrows point at characteristic wavenumbers for the indicated species.

fundamental band gap in films produced by sputtering at high oxygen pressures, which is in disagreement with our results for reasons that are not clear to us.

The spectral absorption characteristics are of importance for understanding the photocatalysis of the films. Specifically we use the relation [36]

$$\alpha(E) \propto \left[1 - \frac{2}{\pi}\tan^{-1}\left[\frac{E_g - E}{\sum}\right]\right], \qquad (2)$$

where $\alpha(E)$ is the absorption coefficient as a function of energy, E_g is the fundamental band gap and expresses the energy around which the transition from low to high absorption is centered, and Σ represents the width of the transition. The above relation is based on an approximation applicable to quantum-mechanical transitions between an initial and a final state, according to time-dependent perturbation theory, and is valid for small Σ.

The fundamental band gap can easily be obtained from the inflection point of the $\alpha(E)$ characteristic inherent in Eq. (2). E_g shifts towards higher energies for increasing Γ, as expected from the corresponding shift of k in Fig. 5. It is also possible to evaluate the width of the transition to high absorption, as given by Σ. Table I shows that this parameter is approximately constant for all of the films, possibly excepting the one deposited at the highest oxygen flow which displayed a somewhat lower Σ.

Equation (2) can be used to provide a good fit to experimental data for energies above E_g but fails for energies below the band gap [33, 36]. In order to complete the analysis of the absorption tail for $E < 3$ eV we then apply the relation [37]

$$\alpha_u(E) = a_o \exp\left[\frac{E - E_o}{\Delta E}\right] \qquad (3)$$

where a_o and E_o are constants characteristics of the material, ΔE is a parameter representing the slope of the exponential tail, known as the Urbach tail, and a_o is a constant; specific values are given in Table I. An increase in ΔE means a widening of the Urbach tail, i.e., the sample deposited at the highest oxygen content shows the lowest Urbach tail. This observation is consistent the narrowing of the transition from low to high absorption implied in Σ of Eq. (2).

We now turn to infrared reflectance spectra of Ti oxide films deposited onto ITO-coated substrates. Measurements were taken in the 400 to 4000 cm^{-1} wavenumber range with a double-beam Perkin-Elmer 983 infrared spectrophotometer equipped with air drier. Reflectance data, indicated as R_p, were obtained with p-polarized light at 60° angle of incidence and using an aluminum mirror as a reference.

Fig. 6 shows spectral infrared reflectance for Ti oxide films prepared by sputtering at different values of Γ. Dips in the reflectance curves correspond to absorption maxima. The features around 3400 cm^{-1} pertain to O–H stretching modes due to H_2O; this absorption is especially distinct for the anatase type film made at $\Gamma = 0.078$. Using the approximation that the transmittance is equal to the square root of the reflectance, the absorption coefficient can be obtained from

$$\alpha_{IR} = -\frac{\ln\left(\sqrt{R_p}\right)}{2d} \qquad (4)$$

The amount of water in the film can then be estimated by use of the calibrated absorption at 3400 cm^{-1} [38]. We found the concentration to be 0.0086 mol/cm^3 for the anatase-type film, and considering a molar volume of 20.5 cm^3 for this structure [39], the molar percentage of water in the film is as large as ∼18%.

A broad absorption band is observed between 1500 and 3800 cm^{-1} for most of the films, which overlaps with the absorption previously used to quantify the water content. The broad absorption is increased in the rutile-like samples made at low magnitudes of Γ. Both water and hydroxyl (OH^-) ions have stretching modes that absorb in the 2900–3800 cm^{-1} range [40, 41], even starting at 2500 cm^{-1} as reported in some work [42], and it is natural to associate at least part of the wide absorption feature with such modes. Oxygen associated with water molecules, as well as hydroxyl ions, may then be responsible for the excess of oxygen observed in the films by RBS.

Sharp absorption peaks corresponding to longitudinal optical (LO) modes of Ti–O bonds were observed at 870 cm^{-1} for the anatase type film deposited at

$\Gamma = 0.078$, and similar features lay at wavenumbers as small as $\sim$830 cm^{-1} for rutile-like films made at lower values of Γ. Our observations are in agreement with the reported LO modes in the rutile phase of TiO_2 [43] which yield absorption centered at 830 cm^{-1}.

5. Data on photo-electrocatalytic degradation of 4-CP

We used Ti oxide films to study the photo-electrocatalytic degradation of 4-CP by using a specially designed reactor. It consists of a cylindrical Teflon container. The open end—which can be irradiated by ultraviolet (UV) light—has provisions for mounting a sample with the Ti oxide film facing the interior of the cylinder. Two parallel quartz windows are arranged at right angles to the cylinder axis so as to allow spectrophotometric transmittance measurements for probing the contents of the cylinder. A three-electrode arrangement was used in the experiments. It includes a Pt foil as counter electrode, a Metrohm Ag/AgCl electrode as reference, and the Ti oxide film as working electrode; all of them are immersed in the 4-CP solution. This set-up was referred to as a "single compartment cell" in earlier work of ours [14]. The photoreactor is described in some detail elsewhere [14].

The experimental data, to be reported below, were obtained with 8 ml of 5×10^{-5} M 4-CP in the container, in a distilled water solution with pH = 5.5. UV irradiation was accomplished by use of an Osram Ultramed 2000 W lamp mounted 28 cm in front of the sample. As found from the technical specification of the lamp, the intensity in the UV-A2 spectrum (315 to 400 nm) was nine times higher than the intensity in the UV-B2 spectrum (280 to 315 nm). The photoreactor was positioned in the sample compartment of a Monolite 6602 spectrophotometer operating at $200 < \lambda < 380$ nm. A mechanical chopper system was employed to avoid UV irradiation during the spectrophotometer recordings. Electrochemical measurements were taken by use of a Schlumberger Solartron 1286 Electrochemical Interface.

An applied bias potential of 0.7 V vs. the Ag/AgCl reference electrode was used to avoid electron–hole recombination in the irradiated samples; this effect may otherwise be significant mainly as a consequence of traps and surface states. In order to diminish the influence of free oxygen, which is a well known electron scavenger, nitrogen bubbles were introduced continuously into the sample compartment so that the solution was kept uniformly mixed.

Reaction products such as benzoquinone (BZ), hydroquinone, chlorocatechol, etc. are expected to appear as a result of the photocatalysis of 4-CP [44, 45]. These products, as well as the 4-CP itself, display characteristic optical absorption so that they can be identified by spectrophotometry. Figs 7a–d show typical absorbance spectra of the 4-CP solution during the photo-electrocatalysis with Ti oxide films prepared at different Γs. The spectral data display pronounced absorption at short wavelengths due to 4-CP. This absorption drops monotonically under UV irradiation concomitantly with an increase of the absorption due to BZ. The later substance is an intermediate of the photo-electrocatalytic degradation of 4-CP to harmless products [14, 44, 45]. Intermediates of the

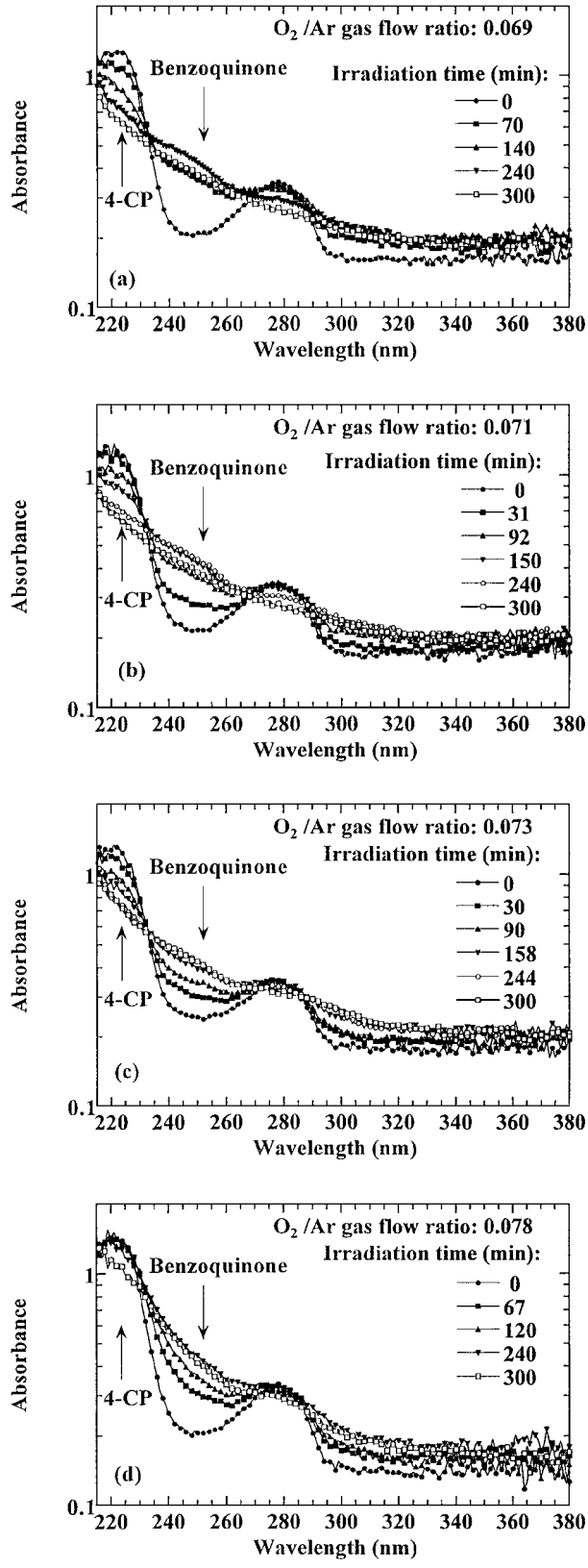

Figure 7 Spectral absorbance measured after UV irradiation for the shown times in order to degrade 5×10^{-5} M 4-CP. Parts (a) to (d) refer to Ti oxide films made by sputtering at the shown O_2/Ar gas flow ratios. Arrows point at characteristic wavelengths for the indicated species.

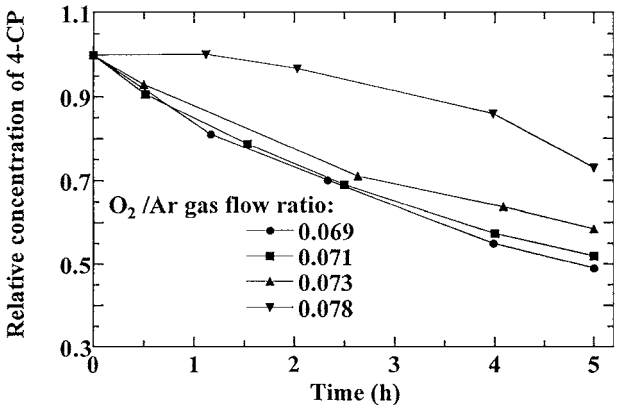

Figure 8 Relative concentration of 4-CP as a function of time for Ti oxide films made by sputtering at the shown O_2/Ar gas flow ratios. Symbols denote data and lines were drawn for convenience.

photo-electrocatalytic degradation, such as the BZ, are expected to increase in concentration at the beginning of the photocatalytic reaction. They are then photodegraded during the photocatalysis in a parallel process [46], so that the absorption reaches a maximum and eventually decreases. This behavior was observed in our case for the feature due to BZ.

Fig. 8 shows the relative concentration of the 4-CP during its photo-electrocatalytic degradation. The data are based on the intensity of the absorption at $\lambda = 225$ nm. It is evident that the thin film fabrication plays an important role for the photodegradation and that its rate is increased in rutile-like films made at low oxygen-to-argon ratios. After 5 h the concentration of the 4-CP in the solution has decreased to half of the initial concentration in the best of the cases. The rate of photocatalytic degradation caused by the rutile-like films is seen to be different than in the case of the anatase-like film. The photo-electrocatalytic degradation rate correlates with the optical absorption at short wavelengths, as evident from Fig. 5. A similar observation was made recently by Mikula *et al*. [13]. Furthermore, we have shown in earlier work of ours [23] that the photoresponse increases in low oxygen content films, which correlates with E_g as well.

We should point out that for the used lamp, the maximum of the irradiation spectra is around 350 nm. Illuminating the films through the substrate will cut off the irradiation below 300 nm mainly due to absorption in the glass. This absorption is overlapping more with the absorption in the anatase than in the rutile. In other words, the rutile-like films will absorb light more efficiently than the anatase-like films.

6. Summary and concluding remarks

We prepared Ti oxide films by reactive magnetron sputtering under conditions known to give "penniform" configurations with high porosity and structural contiguity [22]. Rutile-like and anatase-like films were obtained at low and high oxygen admixture in the sputter plasma respectively, as found from XRD. A small overstoichiometry in oxygen was detected by RBS. Spectrophotometry was used to derive optical constants and analyze the absorption around the fundamental band gap, and IR reflectance spectroscopy gave evidence for water incorporation and OH bonding.

The photo-electrocatalytic ability of the films to degrade 4-CP was investigated in detail in a reactor allowing optical measurements to document the presence of 4-CP as well as the intermediate reaction product BZ. The rutile-like films were capable of decomposing the 4-CP at a higher rates than the anatase-like sample. This can be reconciled with the narrower optical band gap of the rutile structure making it more facile for photoinduced holes to take part in oxidation processes and to the larger amount of OH bound onto its surface.

Acknowledgment

Dr. J. Lindgren is thanked for fruitful discussions and Dr. G. Possnert is acknowledged for his help with RBS measurements. Two of us (M. G. and J. R.) want to thank the International Science Programme at Uppsala University for scholarships.

References

1. N. SERPONE, P. MARUTHAMUTHU, P. PICHAT, E. PELIZZETTI and H. HIDAKA, *J. Photochem. Photobiol. A* **85** (1995) 247.
2. M. R. HOFFMANN, S. T. MARTIN, W. CHOI and D. W. BAHNEMANN, *Chem. Rev.* **95** (1995) 69.
3. A. MILLS and S. LE HUNTE, *J. Photochem. Photobiol. A* **108** (1997) 1.
4. P. SAWUNYAMA, A. FUJISHIMA and K. HASHIMOTO, *Langmuir* **15** (1999) 3551.
5. D. M. BLAKE, in "Bibliography of work on the heterogeneous photocatalytic removal of hazardous compounds from water and air," National Renewable Energy Laboratory, Golden, USA, 1999; internal report.
6. Y. KIKUCHI, K. SUNADA, T. IYODA, K. HASHIMOTO and A. FUJISHIMA, *J. Photochem. Photobiol. A* **106** (1997) 51.
7. H. MATSUBARA, M. TANAKA, S. KOYAMA, K. HASHIMOTO and A. FUJISHIMA, *Chem. Lett.* (1995) 767.
8. Y. PAZ and A. HELLER, *J. Mater. Res.* **12** (1997) 2759.
9. N. SAKAI, R. WANG, A. FUJISHIMA, T. WATANABE and K. HASIMOTO, *Langmuir* **14** (1998) 5918.
10. R. WANG, K. HASHIMOTO and A. FUJISHIMA, *Nature* **388** (1997) 432.
11. B. R. WEINBERGER and R. B. GARBER, *Appl. Phys. Lett.* **66** (1995) 2409.
12. J. SHENG, J. KARASAWA and T. FUKAMI, *J. Mater. Sci. Lett.* **16** (1997) 1709.
13. M. MIKULA, M. CEPPAN and KINDERNAY, *J. Czech. J. Phys.* **49** (1999) 393.
14. J. RODRÍGUEZ, M. GÓMEZ, S.-E. LINDQUIST and C. G. GRANQVIST, *Thin Solid Films* **360** (2000) 250.
15. M. GÓMEZ, J. RODRÍGUEZ, S.-E. LINDQUIST and C. G. GRANQVIST, *ibid.* **342** (1999) 148.
16. K. OKAMOTO, Y. YAMAMOTO, H. TANAKA and A. ITAYA, *Bull. Chem. Soc. Jpn.* **58** (1985) 2015.
17. V. AUGUGLIARIO, L. PALMISANO, A. SCLAFANI, C. MINERO and E. PELIZZETI, *Toxicol. Environ. Chem.* **16** (1988) 89.
18. A. SCLAFANI, L. PALMISANO and M. SCHIAVELLO, *J. Phys. Chem.* **94** (1990) 829.
19. W. CHOI, A. TERMIN and M. R. HOFFMANN, *Angew. Chem. Int. Ed.* **33** (1994) 1091.
20. J. RODRÍGUEZ, M. GÓMEZ, G. A. NIKLASSON and C. G. GRANQVIST, *J. Phys. D: Appl. Phys.* **33** (2000) 24.
21. D. LE BELLAC, G. A. NIKLASSON and C. G. GRANQVIST, *J. Appl. Phys.* **77** (1995) 6145.

22. J. RODRÍGUEZ, M. GÓMEZ, Y. LU, E. OLSSON and C. G. GRANQVIST, *Adv. Mater.* **12** (2000) 341.
23. M. GÓMEZ, J. RODRÍGUEZ, S.-E. LINDQUIST and C. G. GRANQVIST, in Conference Proceedings, EUROSUN 98, Slovenia, September 1998.
24. M. STROMME, A. GUTARRA, G. A. NIKLASSON and C. G. GRANQVIST, *J. Appl. Phys.* **79** (1996) 3749.
25. M. STROMME, J. ISIDORSSON, G. A. NIKLASSON and C. G. GRANQVIST, *ibid.* **80** (1996) 233.
26. L. KULLMAN, A. AZENS and C. G. GRANQVIST, *ibid.* **81** (1997) 8102.
27. POWDER DIFFRACTION FILES (Int. Center for Diffraction Data); files 21-1272 and 21-1276.
28. F. ZHANG and X. LIU, *Thin Solid Films* **326** (1998) 171.
29. M. KIUCHI, A. CHAYAHARA, Y. HORINO, K. FUJII, M. SATOU and W. ENSINGER, *Appl. Surf. Sci.* **60/61** (1992) 760.
30. F. ZHANG, Z. ZHENG, Y. CHEN and X. J. LIU, *Appl. Phys.* **83** (1998) 4101.
31. I. HAMBERG, Ph.D. Thesis, Chalmers University of Technology, Gothenburg, Sweden, 1984 (unpublished).
32. A. R. FOROUHI and I. BLOOMER, in "Handbook of Optical Constants of Solids II," edited by E. D. Palik (Academic, New York, 1991) p. 465.
33. J. RODRÍGUEZ, M. GÓMEZ, J. EDERTH, G. A. NIKLASSON and C. G. GRANQVIST, *Thin Solid Films* **365** (2000) 120.
34. S. BEN AMOR, G. BAUD, J. P. BESSE and M. JACQUET, *ibid.* **293** (1997) 163.
35. *Idem.*, *Mater. Sci. Eng.* **B47** (1997) 110.
36. I. HAMBERG, C. G. GRANQVIST, K.-F BERGGREN, B. E. SERNELIUS and L. ENGSTRÖM, *Phys. Rev. B* **30** (1984) 3240.
37. F. URBACH, *Phys. Rev.* **92** (1953) 1324.
38. D. N. GLEW and N. S. RATH, *Can. J. Chem.* **49** (1971) 837.
39. D. R. LIDE (ed.), "Handbook of Chemistry and Physics," 73rd ed. (CRC, Boca Raton, 1992) p. 4–163.
40. A. RIOU, Y. CUDENNEC and Y. GERAULT, *Mater. Res. Bull.* **25** (1990) 987.
41. M. SCHMIT and H. D. LUTZ, *ibid.* **26** (1991) 605.
42. A. KYLNER, J. LINDGREN and L. STOLT, *J. Electrochem. Soc.* **143** (1996) 2662.
43. M. BASS, E. W. VAN STRYLAND, D. R. WILLIAMS and W. L. WOLFE (eds.), "Handbook of Optics: Devices, Measurements, and Properties," 2nd ed. (McGraw-Hill, New York, 1995), Vol II.
44. K. VINODGOPAL, S. HOTCHANDANI and P. V. KAMAT, *J. Phys. Chem.* **97** (1993) 9040.
45. K. VINODGOPAL, U. STAFFORD, K. A. GRAY and P. V. KAMAT, *ibid.* **98** (1994) 6797.
46. J. THEURICH, M. LINDNER and D. W. BAHNEMANN, *Langmuir* **12** (1996) 6368.

Received 2 June 2000
and accepted 1 February 2001